# Autophagy-mediated degradation of Fatty Acid Synthase (FASN) facilitates ATRA-induced granulocytic differentiation of acute myeloid leukemia (AML) cells

Magali Humbert[1,2,#], Kristina Seiler[1,3], Severin Mosimann[1], Vreni Rentsch[1], Sharon L. McKenna[2,4], Mario P. Tschan[1,2,3]

[1]Institute of Pathology, Division of Experimental Pathology, University of Bern, Bern, Switzerland

[2]TRANSAUTOPHAGY: European network for multidisciplinary research and translation of autophagy knowledge, COST Action CA15138

[3]Graduate School for Cellular and Biomedical Sciences, University of Bern, Bern, Switzerland,

[4]Cancer Research at UCC, Western Gateway Building, University College Cork, Cork, Ireland.

# corresponding author

## Abstract

Acute myeloid leukemia (AML) is a blood cancer characterized by a block in differentiation and increased survival of the resulting AML blast cells. While standard chemotherapy for AML cures only 30% of patients, differentiation-inducing therapy using all-*trans* retinoic acid (ATRA) in combination with arsenic trioxide achieves 90% cure rates in acute promyelocytic leukemia (APL). A better understanding of the molecular mechanisms underlying ATRA therapy in APL may provide new perspectives in the treatment of additional AML subtypes.

Fatty acid synthase (FASN) is the only human lipogenic enzyme available for *de novo* fatty acid synthesis. While FASN levels are very low in healthy adult tissues, it is often highly expressed in cancer cells, thus representing a potential therapeutic target. We found that FASN mRNA levels were significantly higher in AML patients than in healthy granulocytes or $CD34^+$ hematopoietic progenitors in two AML cohorts (n=68, n=203) ($p<0.05$). Accordingly, FASN levels decreased during ATRA-mediated granulocytic differentiation of APL cells, partially via autophagic degradation. Furthermore, our data suggests that inhibition of FASN expression levels using RNAi or (-)-epigallocatechin-3-gallate (EGCG), accelerates the differentiation of APL cell lines and significantly re-sensitized ATRA refractory non-APL AML cells. Decreasing FASN expression reduced mTOR activity and promoted translocation of transcription factor EB (TFEB) to the nucleus. Lysosomal biogenesis was activated, consistent with TFEB transcriptional activation of CLEAR network genes.

Together, our data demonstrates that inhibiting FASN expression in combination with ATRA treatment promotes granulocytic differentiation of APL cells and may extend differentiation therapy to non-APL AML cells.

## Introduction

While traditional chemotherapy and radiotherapy aim to kill highly proliferative cancer cells, differentiation-inducing therapy aims to restore differentiation programs to drive cancer cells into maturation and ultimately into cell death. Differentiation therapies are associated with lower toxicity compared to classical cytotoxic therapies. The success of this therapeutic approach is exemplified by the introduction of all-*trans* retinoic acid (ATRA) in 1985 to treat acute promyelocytic leukemia (APL)[1]. The introduction of ATRA into the treatment regimen changed APL from being one of the most aggressive acute myeloid leukemia (AML) subtypes with a fatal course often within weeks only, to a curable disease with a complete remission rate of up to 95% of patients when combined with anthracycline-based chemotherapy or arsenic trioxide[1]. APL is characterized by translocations involving the C-terminus of the retinoic acid receptor alpha (RARA) on chromosome 17 and genes encoding for aggregate prone proteins. Promyelocytic leukemia (PML)-RARA is the most frequently expressed fusion protein. It is encoded by the translocation t(15;17) and has a dominant negative effect on RARA. RARA transcriptionally regulates multiple biological processes with a key role in differentiation[2]. Several reports suggest a beneficial effect of ATRA in combination therapies in non-APL AML cells[3–5]. Unfortunately, a variety of intrinsic resistance mechanisms in non-APL AML have been identified such as SCL overexpression, expression of PRAME and epigenetic silencing or mutation of RARA[6–9]. Deciphering the mechanisms active during ATRA-mediated differentiation at the molecular level will support the translation of differentiation therapy to non-APL AML patients. We and others have demonstrated the important role of autophagy in ATRA induced granulocytic differentiation of APL cells[10–16]. Autophagy is an intracellular degradation mechanism that ensures dynamic recycling of various cytoplasmic contents[17]. We thus

aim to understand the role of autophagy in granulocytic differentiation and define key druggable autophagy targets in this process.

Endogenous synthesis of fatty acids is catalyzed by fatty acid synthase (FASN), the only human lipogenic enzyme able to perform *de novo* synthesis of fatty acids [18,19]. FASN is frequently overexpressed in a variety of tumor types including leukemias [20–26] while its expression in healthy adult tissues is low[27], with the exception of the cycling endometrium [28] and lactating breast [29]. Interestingly, FASN is upregulated in tumor associated myeloid cells where it activates nuclear receptor peroxisome-proliferator-activated receptor beta/delta (PPARβ/δ)[30], a key metabolic transcription factor in tumorigenesis[31,32]. Of note, activation of PPARβ/δ regulates anti-inflammatory phenotypes of myeloid cells in other biological contexts such as atherosclerosis and obesity[33–36]. We previously reported that (-)-epigallocatechin-3-gallate (EGCG) improved ATRA induced differentiation of APL cells by increasing the expression of death associated protein kinase 2 (DAPK2). Furthermore, EGCG treatment reduces FASN expression levels in selected breast cancer cell lines[37]. The increased FASN expression in cancer including leukemias, its function in tumor-associated myeloid cells and its link to the differentiation enhancer DAPK2 prompted us to analyze the regulation and function of FASN during leukemic differentiation.

In the present study, we demonstrate that FASN expression is significantly higher in AML blasts partially due to low autophagic activity in those cells. We show that inhibiting FASN protein expression, but not enzymatic activity, promotes differentiation of non-APL AML cells. Lastly, we link FASN expression to the inhibition of the key lysosomal biogenesis transcription factor TFEB.

## Material and Methods

### *2.1. Primary cells, cell lines and culture conditions*

Fresh leukemic blast cells from untreated AML patients at diagnosis obtained at the Inselspital Bern (Switzerland) were classified according to the French-American-British classification and cytogenetic analysis. All leukemia samples had blast counts 90% after separation of mononuclear cells using a Ficoll gradient (Lymphoprep; Axon Lab AG, Switzerland), as described previously[38]. Protocols and use of 67 human samples acquired in Bern were approved by the Cantonal Ethical Committee at the Inselspital. The isolation of primary neutrophils (purity 95%) was performed by separating blood cells from healthy donors using polymorphprep (AxonLab AG). $CD34^+$ cells from cord blood or bone marrow were isolated as described[38].

The human AML cell lines, HT93, OCI/AML2, MOLM13 and NB4 were obtained from the Deutsche Sammlung von Mikroorganismen und Zellkulturen GmbH (DSMZ, Braunschweig, Germany). All cell lines were maintained in RPMI-1640 with 10% fetal calf serum (FCS), 50 U/mL penicillin and 50 µg/mL streptomycin in a 5% $CO_2$-95% air humidified atmosphere at 37°C. For ATRA-induced differentiation experiments, cells were treated with 1µM all-*trans* retinoic acid (ATRA; Sigma-Aldrich). Successful granulocyte differentiation was evidenced by CD11b surface expression measured by FACS.

293T cells were maintained in DMEM (Sigma-Aldrich, St. Louis, MO, USA), supplemented with 5% FBS, 1% penicillin/streptomycin, and 1% Hepes (Sigma-Aldrich), and kept in a 7.5%$CO_2$-95% air humidified atmosphere at 37°C.

### *2.2 Antibodies*

Antibodies used were anti-FASN (3180; Cell signaling), anti-LC3B (WB: NB600-1384, Novus biological; IF: 3868; Cell Signaling) anti-LAMP1 (14-1079-80; Thermofisher),

anti-p62 (HPA003196 ;sigma), anti-TFEB (4240; Cell Signaling) anti-ULK1(4776; Cell Signaling), anti p-ULK1 (Ser757) (6888; Cell Signaling), anti-ATG13 (6940 ; Cell Signaling), anti-pATG13 (Ser318) (600-401-C49; Rockland), anti p-mTOR (Ser2448) (5536; Cell Signaling), p4E-BP1 (Thr37/46) (2855; Cell Signaling), anti-α-tubulin (3873; Cell Signaling), anti-cleaved PARP(9541; Cell Signaling), anti yH2AX (2577; Cell Signaling) and anti-CD11b-PE (R0841; Dako).

*2.3 Cell lysate preparation and western blotting*

Whole cell extracts were prepared using UREA lysis buffer and 30-60µg of total protein was loaded on a 7.5% or 12% denaturing polyacrylamide self-cast gel (Bio-Rad). Blots were incubated with the primary antibodies in TBS 0.05% Tween-20 / 5% milk overnight at 4°C and subsequently incubated with HRP coupled secondary goat anti-rabbit (7074; Cell signaling) and goat anti-mouse antibody (7076; Cell signaling) at 1:5–10,000 for 1 h at room temperature. Blots were imaged using the Chemidoc (Bio-Rad) and ImageLab software.

*2.4 Lentiviral vectors*

pLKO.1-puro lentiviral vectors expressing shRNAs targeting *FASN* (sh*FASN*_1: NM_004104.x-1753s1c1 and sh*FASN*_2: NM_004104.x-3120s1c1) were purchased from Sigma-Aldrich. A mCherry-LC3B lentiviral vector was kindly provided by Dr. Maria S. Soengas (CNIO, Molecular Pathology Program, Madrid, Spain). All vectors contain a puromycin antibiotic resistance gene for selection of transduced mammalian cells. Lentivirus production and transduction were done as described[39,40]. Transduced NB4 cell populations were selected with 1.5 µg/ml puromycin for 4 days and knockdown efficiency was assessed by western blot analysis.

*2.5 Immunofluorescence microscopy*

Cells were prepared as previously described[15]. Briefly, cells were fixed and permeabilized with ice-cold 100% methanol for 4 min (LC3B and LAMP1 staining) or 2% paraformaldehyde for 7minutes followed by 5 minutes in PBS TRITONX (TFEB and tubulin staining) and then washed with PBS. Cells were incubated with primary antibody for 1 h at room temperature followed by washing steps with PBS containing 0.1% Tween (PBS-T). Cells were incubated with the secondary antibody (anti-rabbit, 111-605-003 (Alexa Fluor® 647) 111-096-045 (FITC); anti-mouse, (Cy3) 115-605-003 (Alexa Fluor® 647); Jackson ImmunoResearch, West Grove, PA, USA,) for 1 h at room temperature. Prior to mounting in fluorescence mounting medium (S3032; Dako) cells were washed three times with PBS-Tween. Images were acquired on a Olympus FluoView-1000 confocal microscope (Olympus, Volketswil, Switzerland) at x63 magnification.

## 2.6 Acridine Orange staining

Cells were washed 3 times with PBS and resuspended in RPMI 10% FBS containing 5ug/mL Acridine Orange (Invitrogen: A3568) to a concentration of 0.2*106 cells per mL. Cells were then incubated at 37°C for 20minutes and washed 3 times with PBS. Acridine Orange staining was measured by FACS using Laser 488nm with 530/30 (GREEN) and filter 695/40 (RED) filters on a FACS LSR-II (BD). Data were analyzed with FlowJo software. The software derived the RED/GREEN ratio and we compared the distribution of populations using the Overton cumulative histogram subtraction algorithm to provide the percentage of cells more positive than the control.

## 2.7 Nitroblue tetrazolium reduction test

Suspension cells (5 x $10^5$) were resuspended in a 0.2% nitro blue tetrazolium (NBT) solution containing 40ng/ml PMA and incubated 15min at 37°C. Cells were then

washed with PBS, and subjected to cytospin. Counterstaining was done with 0.5% Safranin O for 5min (HT90432; Sigma). The NBT-positive and negative cells were scored under a light microscope (EVOS).

### 2.8 Trypan blue exclusion counting

Trypan blue exclusion cell counting was performed to assess cellular growth. 20µL of cells suspension was incubated with an equal volume of 0.4% (w/v) trypan blue solution (Sigma-Aldrich). Cells were counted using a dual-chamber hemocytometer and a light microscope.

### *2.9 Statistical analysis*

Nonparametric Mann-Whitney-U tests were applied to compare the difference between two groups and Spearman Coefficient Correlation using Prism software. P-values < 0.05 were considered statistically significant.

### 3.1. Primary AML blast cells express significantly higher FASN levels compared to mature granulocytes

Cancer cells frequently express high levels of FASN compared to their healthy counterparts[20–26]. We examined *FASN* mRNA expression in an AML patient cohort with well-defined molecular subtypes. *FASN* mRNA levels in AML samples (n=68) were compared to the levels in granulocytes (n=5) and $CD34^+$ human hematopoietic progenitor cells (n=3) from healthy donors. We found that *FASN* expression was significantly higher in AML patients compared to granulocytes and $CD34^+$ hematopoietic progenitors from healthy donors ($p<0.05$) (Figure 1A). We obtained similar findings by analyzing *FASN* expression in AML patient data available from the Bloodspot gene expression profile data base[41] (Figure 1B). Of note, there were no significant differences in FASN expression in different AML subtypes (data not shown). Next, we asked if FASN expression was altered during granulocytic differentiation of APL cells. We analyzed FASN expression following ATRA-induced differentiation of two APL cell lines, NB4 and HT93. ATRA treatment resulted in markedly reduced FASN protein levels from day two onwards (Figure 1C). This further suggests that high FASN expression is linked to an immature blast-like phenotype and that ATRA-induced differentiation reduces the levels of FASN (Figure 1C).

### 3.2. FASN protein is degraded via macroautophagy during ATRA-induced granulocytic differentiation

We and others have demonstrated that autophagy gene expression is repressed in AML samples compared to granulocytes from healthy donors and that autophagy activity is essential for successful ATRA-induced APL differentiation[10–16,42–44]. The decrease in FASN expression upon ATRA-induced differentiation cannot be explained solely by transcriptional regulation due to the long half-life of this protein (1-3 days)[45,46].

Moreover, FASN can be present inside autophogosomes, for instance in yeast and in the breast cancer cell MCF7[47,48]. Therefore, we hypothesized that ATRA-induced autophagy participates in the degradation of FASN during differentiation of APL cells. To examine whether autophagy is important for degradation of FASN, we treated NB4 cells for 24h with different concentrations of Bafilomycin A1 (BafA1), a specific inhibitor of vacuolar-type $H^+$-ATPase [49,50], alone or in combination with ATRA. FASN protein was found to accumulate in the presence of BafA1, together with autophagy markers p62 and LC3B-II (Figure 2A). To access if FASN degradation is feature of canonical autophagy, we assessed expression during starvation-induced autophagy. NB4 cells were starved for 2 hours using EBSS medium, a time period that induces autophagy without cell death (Supplementary Figure 1). Upon starvation, we detected lower FASN protein levels (Figure 2B). Furthermore, FASN protein levels were slightly stabilized by inhibiting autolysosome formation using BafA1 (200nM) during starvation. This data suggests that FASN may be degraded via canonical autophagy (Figure 2B).

To further assess this possibility, we utilized NB4 cells stably expressing mCherry-LC3B. Cells were treated with different concentrations of BafA1 with or without ATRA for 24h and FASN as well as LC3B localization was assessed. Endogenous FASN (cyan) showed co-localization with mCherry-LC3B (red) in BafA1 and ATRA treated cells (Figure 2C, right panels). In addition, we found colocalization with endogenous FASN (red) and p62 (green) in NB4 parental cells treated with both ATRA and BafA1 for 24h (Figure 2D). It is possible that p62 may help to sequester FASN to the autophagosome – although co-localisation of p62 to the lysosome would be expected. In summary, this data suggests that FASN is a target for autophagic degradation during granulocytic differentiation of APL cells.

We have previously shown that EGCG improves the response to ATRA in AML cells by inducing DAPK2 expression, a key kinase in granulocytic differentiation[51]. Furthermore, EGCG was reported to decrease FASN expression[37] and this was reproducible in our APL cell line model (Supplementary Figure 2A-B). Using different EGCG doses and treatment time points, we confirmed that EGCG improves ATRA induced differentiation in NB4 cells, as evidenced by increased NBT positive cells and CD11b surface expression (Supplementary Figure 2C-E). Autophagic activity was also enhanced (Supplementary Figure 2F-G). Autophagy induction was determined by quantifying endogenous, lipidated LC3B-II by western blotting and a dual-tagged mCherry-GFP-LC3B expression construct as described previously[14,52,53]. Autophagic flux quantification upon EGCG treatment was performed in the presence or absence of BafA1[53]. We found no significant changes in cell death or proliferation measured by DAPI staining and trypan blue exclusion, respectively (Supplementary Figure 2H-I). In addition, by co-treating NB4 parental cells with EGCG and ATRA for 24h and increasing concentrations of BafA1, we clearly demonstrate that EGCG potentiates ATRA induced autophagy, leading to an increase in FASN protein degradation as confirmed by western blotting (Figure 3). Together our data demonstrate that FASN is degraded via autophagy upon ATRA treatment in APL cell lines and that co-treatment with EGCG promotes FASN protein degradation and increases its ubiquitination.

### 3.4. Inhibiting FASN protein expression but not its catalytic function leads to acceleration of ATRA-induced differentiation

Next, we evaluated the impact of modulating FASN expression and activity on myeloid differentiation. Therefore, we genetically inhibited FASN expression using lentiviral vectors expressing 2 independent shRNAs targeting *FASN* in the NB4 APL cell line model. Knockdown efficiency was validated by western blotting (Figure 4A). We found

that ATRA treatment significantly reduced the doubling time (supplementary Figure 3A-B) and lowered accumulation of DNA damage as indicated by yH2AX immunofluorescence staining in NB4 *FASN* depleted cells (Supplementary Figure 3C-D). Of note, at steady state conditions, knocking down *FASN* did not affect proliferation compared to control cells. Knocking down *FASN* in NB4 cells resulted in accelerated differentiation into functional granulocytes compared to the control cells as shown by NBT assays (Figure 4B-C) and by CD11b surface expression analysis (Figure 4D). We then assessed the effects of two pharmacological FASN inhibitors, C75 and Orlistat. We used C75 and Orlistat concentrations that do not induce significant cell death (supplementary Figure 4A-B) or decrease proliferation (Supplementary figure 4C-D) to avoid non-specific results. Of note, FASN protein levels in APL cells were not reduced by C75 or Orlistat treatment (supplementary Figure 4E-F). Unexpectedly, co-treatment of NB4 cells with ATRA and C75 (Figure 4E-G) or Orlistat (Figure 4H-J) did not reproduce the phenotype of the *FASN* knockdown cells. Indeed, cells were differentiating similarly to control cells as demonstrated by the NBT assays (Figure 4E-F and Figure 4H-I) and CD11b surface expression (Figure 4G and Figure 4J). Therefore, we hypothesize that the catalytic activity of FASN is not involved in impeding ATRA-mediated differentiation in NB4 cells.

### 3.5. FASN is a negative regulator of autophagy by increasing mTOR activity

FASN has been previously reported to promote carcinogenesis by activating mTOR, a master negative regulator of autophagy, via AKT in hepatocellular carcinoma[54,55]. ATRA treatment in APL also reduces mTOR activity leading to autophagy activation[56]. We therefore hypothesized that FASN may negatively regulate autophagy via mTOR in APL cells, thereby impeding ATRA-induced differentiation. Therefore, we initially confirmed that FASN expression impacts on autophagic activity in our system. Autophagy induction was determined by quantifying endogenous, lipidated LC3B-II by

western blotting and immunofluorescence microscopy (IF) after ATRA treatment[53]. In order to measure autophagic flux, ATRA treatment was performed in the presence or absence of BafA1[53]. Interestingly, although the autophagy flux ($BafA1^{+}$-$BafA1^{-}$) was not significantly increased based on LC3B-II measurement (Figure 5 A-C), inhibition of FASN protein levels led to a drastic accumulation of p62 upon BafA1 treatment (Figure 5C). Suggesting that FASN expression negatively regulates p62 expression or stability. As LC3B levels are similarly enhanced – it would be consistent with elevation of autophagosomal incorporation of p62 – without lysosomal fusion to degrade it.

ULK1 (ATG1), a key autophagy gene of the initiation complex, is inhibited by mTOR-mediated phosphorylation at Ser757, leading to reduced autophagic activity[57]. In line with FASN activating mTOR, lowering FASN protein expression by shRNA resulted in decreased mTOR-mediated phosphorylation of ULK1 at Ser757. Elevated ULK1 activity was confirmed by an increase of ATG13 phosphorylation at Ser318 mediated by active ULK1[58,59]. These results suggest that FASN expression promotes mTOR activity in AML cells, thereby enhancing its repression of autophagy.

### 3.6. FASN expression negatively affects transcription factor EB (TFEB) activation

mTOR regulates the transcription factor EB (TFEB), a master regulator of lysosome biogenesis)[60,61]. mTOR phosphorylates TFEB, leading to the sequestration of TFEB within the cytoplasm and inhibition of its transcriptional activity[62,63]. TFEB is a key transcriptional regulator of more than 500 genes that comprise the CLEAR (Coordinated Lysosomal Expression and Regulation) network of autophagy and lysosomal genes. A recent study demonstrated the key role of TFEB during ATRA induced differentiation[44]. We therefore investigated the relationship between FASN and CLEAR network gene expression. Interestingly, the majority of the TFEB

downstream targets from the different categories (Lysosomal hydrolases and accessory proteins, Lysosomal membrane, Lysosomal acidification, Non-lysosomal proteins involved in lysosomal biogenesis and autophagy) are negatively associated with FASN transcript levels in primary AML patient blasts from the TCGA analyzed using the UCSC Xena platform[64] and the Blood spot gene expression profiles data base[41] (Supplementary Figure 5, Figure 6A, Supplementary Table 1-2). Furthermore, analyzing RNA-seq data of NB4 cells treated with ATRA confirmed a reduction of FASN expression paralleled by increased TFEB and TFEB target gene transcripts levels[44] (Figure 6B). To test if the FASN-mTOR pathway is involved in regulating TFEB activity, we analyzed the cellular localization of TFEB upon ATRA treatment in NB4 control and FASN depleted cells. First, we investigated if TFEB translocates to the nucleus following ATRA treatment and if this translocation is paralleled by an increase in lysosome numbers ($LAMP1^+$ dots), assessed by immunofluorescence microscopy (Supplementary Figure 6A-B). Indeed, ATRA treatment resulted in increased $LAMP1^+$dot formation and nuclear translocation of TFEB. Interestingly, TFEB nuclear translocation occurs faster in FASN depleted NB4 cells compared to control cells (Figure 6C), consistent with an increase in $LAMP1^+$ dot formation (Figure 6D-E). Furthermore, we treated cells with Acridine Orange to quantify the lysosomal integrity by flow cytometry. Acridine Orange is a cell permeable fluorescent dye that, when excited at 488nm, emits light at 530nm (GREEN) in its monomeric form but shifts its emission to 680nm (RED) when accumulating and precipitating inside lysosomes. Therefore, we measured the RED/GREEN ratio of Acridine Orange stained cells by flow cytometry as previously described[65]. We found that ATRA treatment shifted the ratio towards the red channel (Supplementary Figure 6C). Reducing FASN expression further accelerated the increase of RED/GREEN ratio indicating enhanced lysosome biogenesis (Figure 6 G-H).

These results suggest that FASN expression impairs TFEB translocation to the nucleus and therefore reduces lysosome biogenesis. Next, we tested whether we can obtain similar results by treating the cells with EGCG instead of knocking down *FASN*. Using different EGCG concentrations, we found a decrease in mTOR phosphorylation (Figure 7A), an increase of TFEB translocation to the nucleus (Figure 7B), an increase of LAMP1$^{+}$ vesicles (Figure 7C-D) and an increase of the RED/GREEN ratio in Acridine Orange stained cells similar to the results seen in the FASN depleted APL cells (Figure 7E-G).

Together, these data suggest that high FASN expression results in lower autophagic activity and decreased lysosomal capacity due to increased mTOR activity and inhibition of TFEB.

### 3.7. Lowering FASN expression improves ATRA therapy in non-APL AML cell lines by inhibiting the mTOR pathway

Given the fact that APL cells treated with EGCG demonstrated improved response to ATRA therapy, we asked if EGCG can be beneficial to other AML subtypes that are refractory to ATRA treatment. We and others previously demonstrated a positive impact of co-treating HL60 AML cells, a non-APL AML cell line that responds to ATRA, with EGCG and ATRA. Therefore, we tested if additional ATRA refractory AML cell lines with different genetic backgrounds; MOLM13 (FLT3-ITD$^{+}$) and OCI/AML2 (DNMT3A R635W mutation) would respond to ATRA in combination with EGCG. Both cell lines showed increased granulocytic differentiation upon the combination treatment as shown by CD11b surface expression (Figure 8 A-B). In addition, MOLM-13 and OCI/AML2 showed an increase of RED/GREEN ratio when stained with Acridine Orange (Figure 8C-F) together with a decrease in mTOR activity as seen by a decrease in mTOR (Ser2448) and ULK1 (Ser757) phosphorylation paralleled by an

increase of ATG13 (Ser318) phosphorylation (Figure 8G-H). We further confirmed these data by genetically inhibiting *FASN* in MOLM-13 (Figure 8I) and OCI/AML2 (Figure 8J) cells. Depleting FASN in both cell lines caused an increase of CD11b surface expression after 3 days of ATRA treatment (Figure 8K-L), coupled with an increased RED/GREEN ratio when stained for Acridine Orange (Figure 8M-P) and lower mTOR activity (Figure 8Q-R). Interestingly, we found more variation in lysosomal compartment changes between the experimental duplicates upon ATRA when cells were treated with EGCG (Figure 8D and F) than in the knockdown cells (Figures 8N and 8P), reflecting the side effect of EGCG.

Together, this data suggests that reducing FASN expression can increase lysosomal biogenesis and improve the differentiation of non-APL AML cells.

## Discussion

In this study, we aimed to further dissect the function of fatty acid synthase in AML cells and in particular, its potential role in the differentiation of immature blasts. We showed that knocking down *FASN* accelerated ATRA-induced differentiation, while inhibition of its enzymatic function by pharmacological inhibitors such as C75 or Orlistat had no effect. Furthermore, we found that FASN expression activates mTOR resulting in sequestration of TFEB to the cytoplasm. Importantly, inhibiting *FASN* expression, in combination with ATRA treatment, improved differentiation therapy in non-APL AML cells.

Several studies demonstrated a tumor suppressor role of autophagy in AML cells. Autophagy can support degradation of leukemic oncogenes in AML such as FLT3-ITD and PML-RARA[56,66,67]. Furthermore, activation of mTORC1 is crucial for leukemia cell proliferation at least partially due to its inhibitory effect on autophagy[42,68]. Accordingly, inhibition of autophagy leads to acceleration of MLL-ENL AML leukemia progression *in vivo*[42]. Our results indicate that increased FASN expression in AML might be a key activator of mTORC1. Surprisingly, we found that reducing FASN protein levels, but not inhibition of catalytic function, promotes ATRA-induced differentiation. Recently, Bueno *et al.* demonstrated that FASN is key during the transformation from 2- to 3-dimensional growth of cancer cells. This transformation step does not depend on the FASN biosynthetic products palmitate, further hinting to important non-catalytic functions of FASN in the cancer phenotype[69]. Further studies on the interplay between FASN, mTOR and autophagy in AML transformation, progression and therapy resistance are warranted to improve our understanding of cell fate decisions and could potentially open new avenues to tackle this disease with improved differentiation therapies.

We further confirmed that EGCG positively impacts cellular differentiation in additional AML subtypes *in vitro*[51,70,71]. Searching for potential mediators of the positive effects of EGCG observed during ATRA-induced differentiation, we previously found that EGCG induces expression of the $Ca^{2+}$/calmodulin-regulated serine/threonine kinase DAPK2. DAPK2 plays a major role in granulocytic differentiation and decreased DAPK2 expression in APL cells can be restored by ATRA and EGCG treatment[14,39,51,72]. DAPK2 also negatively regulates mTOR via phosphorylation of raptor at Ser721 as shown in HeLa cells[73]. Therefore, it would be of interest to study the impact of FASN on DAPK2 activity in a leukemic context as well.

Interestingly, treating APL cells with ATRA had a negative effect on FASN protein levels (Figure 1C) and we demonstrated that ATRA-induced autophagy contributes to FASN protein degradation. Furthermore, FASN reduction led to increased lysosomal biogenesis suggesting a negative feedback loop between autophagy and FASN. It is reasonable to hypothesize that the more AML cells differentiate the more they become competent to degrade long-lived proteins including FASN. We and others demonstrated the importance of functional autophagy pathways during ATRA-induced differentiation [10–16,42–44]. In addition inhibiting mTOR using Rapamycin or Everolimus accelerates differentiation of APL cells[13,56]. While PI3K/Akt/mTOR pathways are activated in about 80% of AML cases, mTOR inhibitors had only modest effects in AML therapy[74,75]. Furthermore, despite its role in leukemia cells, mTOR activity is crucial for hematopoietic stem cell proliferation and self-renewal potential[76]. Therefore, targeting FASN that is low expressed in healthy cells would allow activation of autophagy in AML cells, resulting in an increased degradation of long-lived proteins, sparing healthy cells in the bone marrow. EGCG in our hands demonstrated a partial effect compared to the knock down. Therefore, a more specific FASN expression inhibitor will help to improve differentiation therapy in non-APL AML patients.

Indeed, it would be of interest to study the transcriptional regulation of FASN to influence its expression in autophagy deficient cells. Consistently, there are several studies showing that *FASN* transcription is positively affected by retinoic acids[77,78]. However, transcription induction is not mediated by a classic retinoic acid responsive element (RARE) but rather by indirect influence of retinoic acid via *cis*-regulatory elements. Since this involves different cofactors it is tempting to speculate that transcriptional activation might switch to repression depending on the cellular context including specific retinoid-binding proteins and cofactors. We previously found that members of the KLF transcription factor family are often deregulated in primary AML patient samples. Among the different KLFs inhibited in AML, particularly *KLF5* turned out to be essential for granulocytic differentiation[79–81]. KLF5 forms a transcriptionally active complex with RAR/RXR heterodimers[82,83]. Interestingly, ectopic expression of KLF5 in U937 non-APL AML cell line is enough to significantly increase ATRA-induced differentiation[84]. KLFs activity varies depending on the cellular context and the binding partners. Therefore, one can hypothesize that KLF5 in AML cells is a negative regulator of *FASN* expression.

In summary, our data suggest that inducing FASN protein degradation is likely to be beneficial for differentiation therapy of non-APL AML cells as this will impede mTOR and promote TFEB transcriptional activity and autophagy. Furthermore, high FASN expression in AML is likely due to impaired autophagy activity.

## Acknowledgments

Deborah Shan-Krauer is gratefully acknowledged for excellent technical support. We thank Dr. MS Soengas for providing an mCherry-LC3B lentiviral vector. This study was supported by grants from Swiss Cancer Research (KFS-3409-02-2014 to MPT, MD-PhD 03/17 Scholarship to KS), the Swiss National Science Foundation (31003A_173219 to MPT), the Berne University Research Foundation (45/2018, to MPT), the University of Bern initiator grant, the Bernese Cancer League, “Stiftung für klinisch-experimentelle Tumorforschung” , and the Werner and Hedy Berger-Janser Foundation for Cancer Research (to MH). SMCK is supported by Breakthrough Cancer Research.

## Author Contribution

MH, KS, SM, and VR performed the experimental research. MH, KS, SMCK and MPT drafted the article. MH designed the project. MPT gave final approval of the submitted manuscript.

## References

1. Wang, Z.-Y. & Chen, Z. Acute promyelocytic leukemia: from highly fatal to highly curable. *Blood* **111**, 2505–2515 (2008).
2. Germain, P. *et al.* International Union of Pharmacology. LX. Retinoic acid receptors. *Pharmacol. Rev.* **58**, 712–725 (2006).
3. Su, M. *et al.* All-Trans Retinoic Acid Activity in Acute Myeloid Leukemia: Role of Cytochrome P450 Enzyme Expression by the Microenvironment. *PLOS ONE* **10**, e0127790 (2015).

4. Marchwicka, A., Cebrat, M., Sampath, P., Śnieżewski, Ł. & Marcinkowska, E. Perspectives of Differentiation Therapies of Acute Myeloid Leukemia: The Search for the Molecular Basis of Patients' Variable Responses to 1,25-Dihydroxyvitamin D and Vitamin D Analogs. *Front. Oncol.* **4**, (2014).
5. Schenk, T. *et al.* Inhibition of the LSD1 (KDM1A) demethylase reactivates the all-trans-retinoic acid differentiation pathway in acute myeloid leukemia. *Nat. Med.* **18**, 605–611 (2012).
6. Rice, A. M., Holtz, K. M., Karp, J., Rollins, S. & Sartorelli, A. C. Analysis of the relationship between Scl transcription factor complex protein expression patterns and the effects of LiCl on ATRA-induced differentiation in blast cells from patients with acute myeloid leukemia. *Leuk. Res.* **28**, 1227–1237 (2004).
7. Bullinger, L. *et al.* PRAME-induced inhibition of retinoic acid receptor signaling-mediated differentiation--a possible target for ATRA response in AML without t(15;17). *Clin. Cancer Res. Off. J. Am. Assoc. Cancer Res.* **19**, 2562–2571 (2013).
8. Petrie, K., Zelent, A. & Waxman, S. Differentiation therapy of acute myeloid leukemia: past, present and future. *Curr. Opin. Hematol.* **16**, 84–91 (2009).
9. Altucci, L. & Gronemeyer, H. The promise of retinoids to fight against cancer. *Nat. Rev. Cancer* **1**, 181–193 (2001).
10. Isakson, P., Bjørås, M., Bøe, S. O. & Simonsen, A. Autophagy contributes to therapy-induced degradation of the PML/RARA oncoprotein. *Blood* **116**, 2324–2331 (2010).
11. Wang, Z. *et al.* Autophagy regulates myeloid cell differentiation by p62/SQSTM1-mediated degradation of PML-RARα oncoprotein. *Autophagy* **7**, 401–411 (2011).

12. Orfali, N., McKenna, S. L., Cahill, M. R., Gudas, L. J. & Mongan, N. P. Retinoid receptor signaling and autophagy in acute promyelocytic leukemia. *Exp. Cell Res.* **324**, 1–12 (2014).
13. Jin, J. *et al.* Low Autophagy (ATG) Gene Expression Is Associated with an Immature AML Blast Cell Phenotype and Can Be Restored during AML Differentiation Therapy. *Oxid. Med. Cell. Longev.* **2018**, 1482795 (2018).
14. Humbert, M., Federzoni, E. A. & Tschan, M. P. Distinct TP73-DAPK2-ATG5 pathway involvement in ATO-mediated cell death versus ATRA-mediated autophagy responses in APL. *J. Leukoc. Biol.* **102**, 1357–1370 (2017).
15. Brigger, D., Proikas-Cezanne, T. & Tschan, M. P. WIPI-dependent autophagy during neutrophil differentiation of NB4 acute promyelocytic leukemia cells. *Cell Death Dis.* **5**, e1315 (2014).
16. Brigger, D., Torbett, B. E., Chen, J., Fey, M. F. & Tschan, M. P. Inhibition of GATE-16 attenuates ATRA-induced neutrophil differentiation of APL cells and interferes with autophagosome formation. *Biochem. Biophys. Res. Commun.* **438**, 283–288 (2013).
17. Feng, Y., He, D., Yao, Z. & Klionsky, D. J. The machinery of macroautophagy. *Cell Res.* **24**, 24–41 (2014).
18. Asturias, F. J. *et al.* Structure and molecular organization of mammalian fatty acid synthase. *Nat. Struct. Mol. Biol.* **12**, 225–232 (2005).
19. Maier, T., Jenni, S. & Ban, N. Architecture of mammalian fatty acid synthase at 4.5 \AA resolution. *Science* **311**, 1258–1262 (2006).
20. Pizer, E. S., Lax, S. F., Kuhajda, F. P., Pasternack, G. R. & Kurman, R. J. Fatty acid synthase expression in endometrial carcinoma. *Cancer* **83**, 528–537 (1998).
21. Visca, P. *et al.* Fatty acid synthase (FAS) is a marker of increased risk of recurrence in lung carcinoma. *Anticancer Res.* **24**, 4169–4173 (2004).

22. Bandyopadhyay, S. *et al.* FAS expression inversely correlates with PTEN level in prostate cancer and a PI 3-kinase inhibitor synergizes with FAS siRNA to induce apoptosis. *Oncogene* **24**, 5389–5395 (2005).
23. Alo, P. L. *et al.* Expression of fatty acid synthase (FAS) as a predictor of recurrence in stage I breast carcinoma patients. *Cancer* **77**, 474–482 (1996).
24. Shurbaji, M. S., Kalbfleisch, J. H. & Thurmond, T. S. Immunohistochemical detection of a fatty acid synthase (OA-519) as a predictor of progression of prostate cancer. *Hum. Pathol.* **27**, 917–921 (1996).
25. Rashid, A. *et al.* Elevated expression of fatty acid synthase and fatty acid synthetic activity in colorectal neoplasia. *Am. J. Pathol.* **150**, 201–208 (1997).
26. Diaz-Blanco, E. *et al.* Molecular signature of CD34(+) hematopoietic stem and progenitor cells of patients with CML in chronic phase. *Leukemia* **21**, 494–504 (2007).
27. Weiss, L. *et al.* Fatty-acid biosynthesis in man, a pathway of minor importance. Purification, optimal assay conditions, and organ distribution of fatty-acid synthase. *Biol. Chem. Hoppe. Seyler* **367**, 905–912 (1986).
28. Pizer, E. S., Kurman, R. J., Pasternack, G. R. & Kuhajda, F. P. Expression of fatty acid synthase is closely linked to proliferation and stromal decidualization in cycling endometrium. *Int. J. Gynecol. Pathol. Off. J. Int. Soc. Gynecol. Pathol.* **16**, 45–51 (1997).
29. Maningat, P. D. *et al.* Gene expression in the human mammary epithelium during lactation: the milk fat globule transcriptome. *Physiol. Genomics* **37**, 12–22 (2009).
30. Park, J. *et al.* M-CSF from Cancer Cells Induces Fatty Acid Synthase and PPARβ/δ Activation in Tumor Myeloid Cells, Leading to Tumor Progression. *Cell Rep.* **10**, 1614–1625 (2015).

31. Peters, J. M. & Gonzalez, F. J. Sorting out the functional role(s) of peroxisome proliferator-activated receptor-β/δ (PPARβ/δ) in cell proliferation and cancer. *Biochim. Biophys. Acta BBA - Rev. Cancer* **1796**, 230–241 (2009).
32. Zuo, X. *et al.* Targeted Genetic Disruption of Peroxisome Proliferator–Activated Receptor-δ and Colonic Tumorigenesis. *JNCI J. Natl. Cancer Inst.* **101**, 762–767 (2009).
33. Han Jung-Kyu *et al.* Peroxisome Proliferator–Activated Receptor-δ Agonist Enhances Vasculogenesis by Regulating Endothelial Progenitor Cells Through Genomic and Nongenomic Activations of the Phosphatidylinositol 3-Kinase/Akt Pathway. *Circulation* **118**, 1021–1033 (2008).
34. Kang, K. *et al.* Adipocyte-Derived Th2 Cytokines and Myeloid PPARδ Regulate Macrophage Polarization and Insulin Sensitivity. *Cell Metab.* **7**, 485–495 (2008).
35. Lee, C.-H. *et al.* Transcriptional Repression of Atherogenic Inflammation: Modulation by PPARδ. *Science* **302**, 453–457 (2003).
36. Odegaard, J. I. *et al.* Alternative M2 Activation of Kupffer Cells by PPARδ Ameliorates Obesity-Induced Insulin Resistance. *Cell Metab.* **7**, 496–507 (2008).
37. Yeh, C. W., Chen, W. J., Chiang, C. T., Lin-Shiau, S. Y. & Lin, J. K. Suppression of fatty acid synthase in MCF-7 breast cancer cells by tea and tea polyphenols: a possible mechanism for their hypolipidemic effects. *Pharmacogenomics J.* **3**, 267 (2003).
38. Federzoni, E. A. *et al.* PU.1 is linking the glycolytic enzyme HK3 in neutrophil differentiation and survival of APL cells. *Blood* **119**, 4963–4970 (2012).
39. Rizzi, M. *et al.* The death-associated protein kinase 2 is up-regulated during normal myeloid differentiation and enhances neutrophil maturation in myeloid leukemic cells. *J. Leukoc. Biol.* **81**, 1599–1608 (2007).

40. Tschan, M. P. *et al.* Alternative splicing of the human cyclin D-binding Myb-like protein (hDMP1) yields a truncated protein isoform that alters macrophage differentiation patterns. *J. Biol. Chem.* **278**, 42750–42760 (2003).
41. Bagger, F. O. *et al.* BloodSpot: a database of gene expression profiles and transcriptional programs for healthy and malignant haematopoiesis. *Nucleic Acids Res.* **44**, D917–D924 (2016).
42. Watson, A. S. *et al.* Autophagy limits proliferation and glycolytic metabolism in acute myeloid leukemia. *Cell Death Discov.* **1**, (2015).
43. Orfali, N. *et al.* Induction of autophagy is a key component of all-trans-retinoic acid-induced differentiation in leukemia cells and a potential target for pharmacologic modulation. *Exp. Hematol.* **43**, 781-793.e2 (2015).
44. Orfali, N. *et al.* All-trans retinoic acid (ATRA) induced TFEB expression is required for myeloid differentiation in acute promyelocytic leukemia (APL). *Eur. J. Haematol.* (2019) doi:10.1111/ejh.13367.
45. Weiss, L. *et al.* Fatty-acid biosynthesis in man, a pathway of minor importance. Purification, optimal assay conditions, and organ distribution of fatty-acid synthase. *Biol. Chem. Hoppe. Seyler* **367**, 905–912 (1986).
46. Volpe, J. J. & Vagelos, P. R. Mechanisms and regulation of biosynthesis of saturated fatty acids. *Physiol. Rev.* **56**, 339–417 (1976).
47. Dengjel, J. *et al.* Identification of Autophagosome-associated Proteins and Regulators by Quantitative Proteomic Analysis and Genetic Screens. *Mol. Cell. Proteomics MCP* **11**, (2012).
48. Suzuki, K. *et al.* Proteomic Profiling of Autophagosome Cargo in Saccharomyces cerevisiae. *PLOS ONE* **9**, e91651 (2014).

49. Yamamoto, A. *et al.* Bafilomycin A1 prevents maturation of autophagic vacuoles by inhibiting fusion between autophagosomes and lysosomes in rat hepatoma cell line, H-4-II-E cells. *Cell Struct. Funct.* **23**, 33–42 (1998).

50. Poole, B. & Ohkuma, S. Effect of weak bases on the intralysosomal pH in mouse peritoneal macrophages. *J. Cell Biol.* **90**, 665–669 (1981).

51. Britschgi, A., Simon, H.-U., Tobler, A., Fey, M. F. & Tschan, M. P. Epigallocatechin-3-gallate induces cell death in acute myeloid leukaemia cells and supports all-trans retinoic acid-induced neutrophil differentiation via death-associated protein kinase 2. *Br. J. Haematol.* **149**, 55–64 (2010).

52. Gump, J. M. & Thorburn, A. Sorting cells for basal and induced autophagic flux by quantitative ratiometric flow cytometry. *Autophagy* **10**, 1327–1334 (2014).

53. Klionsky, D. J. *et al.* Guidelines for the use and interpretation of assays for monitoring autophagy (3rd edition). *Autophagy* **12**, 1–222 (2016).

54. Hu, J. *et al.* Co-activation of AKT and c-Met triggers rapid hepatocellular carcinoma development via the mTORC1/FASN pathway in mice. *Sci. Rep.* **6**, 20484 (2016).

55. Calvisi, D. F. *et al.* Increased lipogenesis, induced by AKT-mTORC1-RPS6 signaling, promotes development of human hepatocellular carcinoma. *Gastroenterology* **140**, 1071–1083 (2011).

56. Isakson, P., Bjørås, M., Bøe, S. O. & Simonsen, A. Autophagy contributes to therapy-induced degradation of the PML/RARA oncoprotein. *Blood* **116**, 2324–2331 (2010).

57. Kim, J., Kundu, M., Viollet, B. & Guan, K.-L. AMPK and mTOR regulate autophagy through direct phosphorylation of Ulk1. *Nat. Cell Biol.* **13**, 132–141 (2011).

58. Joo, J. H. *et al.* Hsp90-Cdc37 Chaperone Complex Regulates Ulk1- and Atg13-Mediated Mitophagy. *Mol. Cell* **43**, 572–585 (2011).

59. Petherick, K. J. *et al.* Pharmacological Inhibition of ULK1 Kinase Blocks Mammalian Target of Rapamycin (mTOR)-dependent Autophagy. *J. Biol. Chem.* **290**, 11376–11383 (2015).

60. Roczniak-Ferguson, A. *et al.* The transcription factor TFEB links mTORC1 signaling to transcriptional control of lysosome homeostasis. *Sci. Signal.* **5**, ra42 (2012).

61. Napolitano, G. *et al.* mTOR-dependent phosphorylation controls TFEB nuclear export. *Nat. Commun.* **9**, 3312 (2018).

62. Vega-Rubin-de-Celis, S., Peña-Llopis, S., Konda, M. & Brugarolas, J. Multistep regulation of TFEB by MTORC1. *Autophagy* **13**, 464–472 (2017).

63. Peña-Llopis, S. *et al.* Regulation of TFEB and V-ATPases by mTORC1. *EMBO J.* **30**, 3242–3258 (2011).

64. Goldman, M. *et al.* The UCSC Xena platform for public and private cancer genomics data visualization and interpretation. *bioRxiv* 326470 (2019) doi:10.1101/326470.

65. Thomé, M. P. *et al.* Ratiometric analysis of Acridine Orange staining in the study of acidic organelles and autophagy. *J. Cell Sci.* **129**, 4622–4632 (2016).

66. Larrue, C. *et al.* Proteasome inhibitors induce FLT3-ITD degradation through autophagy in AML cells. *Blood* **127**, 882–892 (2016).

67. Rudat, S. *et al.* RET-mediated autophagy suppression as targetable co-dependence in acute myeloid leukemia. *Leukemia* **32**, 2189–2202 (2018).

68. Hoshii, T. *et al.* mTORC1 is essential for leukemia propagation but not stem cell self-renewal. *J. Clin. Invest.* **122**, 2114–2129 (2012).

69. Bueno, M. J. *et al.* Essentiality of fatty acid synthase in the 2D to anchorage-independent growth transition in transforming cells. *Nat. Commun.* **10**, 5011 (2019).

70. Moradzadeh, M., Roustazadeh, A., Tabarraei, A., Erfanian, S. & Sahebkar, A. Epigallocatechin-3-gallate enhances differentiation of acute promyelocytic leukemia cells via inhibition of PML-RARα and HDAC1. *Phytother. Res. PTR* **32**, 471–479 (2018).

71. Lung, H. L. *et al.* Anti-proliferative and differentiation-inducing activities of the green tea catechin epigallocatechin-3-gallate (EGCG) on the human eosinophilic leukemia EoL-1 cell line. *Life Sci.* **72**, 257–268 (2002).

72. Humbert, M. *et al.* The tumor suppressor gene DAPK2 is induced by the myeloid transcription factors PU.1 and C/EBPα during granulocytic differentiation but repressed by PML-RARα in APL. *J. Leukoc. Biol.* **95**, 83–93 (2014).

73. Ber, Y. *et al.* DAPK2 is a novel regulator of mTORC1 activity and autophagy. *Cell Death Differ.* **22**, 465–475 (2015).

74. Mirabilii, S. *et al.* Biological Aspects of mTOR in Leukemia. *Int. J. Mol. Sci.* **19**, (2018).

75. Tabe, Y., Tafuri, A., Sekihara, K., Yang, H. & Konopleva, M. Inhibition of mTOR kinase as a therapeutic target for acute myeloid leukemia. *Expert Opin. Ther. Targets* **21**, 705–714 (2017).

76. Ghosh, J. & Kapur, R. Regulation of Hematopoietic Stem Cell Self-Renewal and Leukemia Maintenance by the PI3K-mTORC1 Pathway. *Curr. Stem Cell Rep.* **2**, 368–378 (2016).

77. Roder, K., Wolf, S. S. & Schweizer, M. Regulation of the fatty acid synthase promoter by retinoic acid. *Biochem. Soc. Trans.* **24**, 233S (1996).

78. Roder, K. & Schweizer, M. Retinoic acid-mediated transcription and maturation of SREBP-1c regulates fatty acid synthase via cis-elements responsible for nutritional regulation. *Biochem. Soc. Trans.* **35**, 1211–1214 (2007).

79. Humbert, M. *et al.* Deregulated expression of Kruppel-like factors in acute myeloid leukemia. *Leuk. Res.* **35**, 909–913 (2011).

80. Diakiw, S. M. *et al.* The granulocyte-associated transcription factor Krüppel-like factor 5 is silenced by hypermethylation in acute myeloid leukemia. *Leuk. Res.* **36**, 110–116 (2012).

81. Li, C. *et al.* MicroRNA-21 promotes proliferation in acute myeloid leukemia by targeting Krüppel-like factor 5. *Oncol. Lett.* **18**, 3367–3372 (2019).

82. Lv, X.-R. *et al.* Synthetic retinoid Am80 up-regulates apelin expression by promoting interaction of RARα with KLF5 and Sp1 in vascular smooth muscle cells. *Biochem. J.* **456**, 35–46 (2013).

83. Kada, N. *et al.* Acyclic retinoid inhibits functional interaction of transcription factors Krüppel-like factor 5 and retinoic acid receptor-alpha. *FEBS Lett.* **582**, 1755–1760 (2008).

84. Shahrin, N. H., Diakiw, S., Dent, L. A., Brown, A. L. & D'Andrea, R. J. Conditional knockout mice demonstrate function of Klf5 as a myeloid transcription factor. *Blood* **128**, 55–59 (2016).

85. Schläfli, A. M., Berezowska, S., Adams, O., Langer, R. & Tschan, M. P. Reliable LC3 and p62 autophagy marker detection in formalin fixed paraffin embedded human tissue by immunohistochemistry. *Eur. J. Histochem. EJH* **59**, 2481 (2015).

Figure Legends

**Figure 1**: Increased FASN expression is associated with an immature AML blast phenotype. A. FASN mRNA levels in AML blasts, $CD34^+$ progenitors cells and granulocyte from healthy donor were quantified by qPCR. All the samples were obtained from the Inselspital, Bern, Switzerland. AML patient cells and granulocytes were isolated using Ficoll gradient density centrifugation. Values are the differences in Ct-values between FASN and the housekeeping gene and ABL1. B. Blood spot data bank analysis of FASN expression in AML blasts compared to granulocytes from healthy donors. MNW * $p<0.05$, ** $p<0.01$. C. Western blot analysis of FASN regulation in NB4 and HT93 APL cells upon ATRA treatment at different time points (1, 2 and 3 days). Total protein was extracted and submitted to immunoblotting using anti-FASN antibody. Total protein is shown as loading control. The relative protein expressions were normalized to total protein and quantified using ImageJ software (NIH, Bethesda, MD, USA).

**Figure 2**: FASN is degraded via autophagy. A. NB4 cells were treated with ATRA and different concentration of Bafilomycin A1 (BafA1) for 24h. NB4 cells were lysed and subjected to western blot analysis as described in 1C. B. NB4 cells were starved using EBSS and treated with different concentrations of Bafilomycin A1 (BafA1) for 2h. NB4 cells were lysed and subjected to western blot analysis. C. NB4 cells stably expressing mCherry-LC3B were treated with ATRA and different concentrations of Bafilomycin A1 (BafA1) for 24h. NB4 mCherry-LC3B cells were fixed and stained for endogenous FASN. The colocalization analysis was performed using ImageJ software. D. NB4 cells were treated as in 2C and fixed and stained for endogenous FASN and p62. The colocalization analysis was performed using ImageJ software.

**Figure 3**: EGCG potentiate ATRA-induced FASN degradation by autophagy. FASN and p62 western blot analysis of NB4 cells treated with DMSO or ATRA, in combination with different EGCG (5µM to 15µM) and BafA1 (1-100nm) concentrations for 24h. Total cell lysates were subjected to western blotting.

**Figure 4**: Reducing FASN protein levels improves ATRA-mediated neutrophil differentiation of APL cells. (A-D). NB4 cells were stably transduced with non-targeting shRNA (SHC002) or shRNAs targeting *FASN* (sh*FASN*_1 and sh*FASN*_2) lentiviral vectors and differentiated with 1µM ATRA for 1, 2 or 3 days. A. FASN western blot analysis of control and sh*FASN* (sh*FASN*_1, _2) expressing NB4 cell populations. B-C. NBT reduction in ATRA-treated NB4 control (SHC002) and *FASN* knockdown (sh*FASN*_1, _2) cells. B. Representative images of NBT assays in control and FASN depleted NB4 cells. C. Quantification of the percentage of $NBT^+$ cells. D. Flow cytometry analysis of CD11b surface expression NB4 control (SHC002) and *FASN* knockdown (sh*FASN*_1, _2) NB4 cells upon ATRA treatment. E-G. NB4 cells were treated with the indicated C75 concentrations for 3 days in combination with ATRA. E-F. NBT reduction during ATRA-mediated neutrophil differentiation of NB4 control and C75 treated cells. E. Representative images of NBT assays in control and C75 treated NB4 cells upon ATRA-mediated differentiation. F. Quantification of the percentage of $NBT^+$ cells. G. Flow cytometry analysis of CD11b surface expression in NB4 control and C75 treated cells upon ATRA-mediated differentiation. H-J. NB4 cells were treated with the indicated Orlistat concentrations for 3 days in combination with ATRA. H-I. NBT reduction during ATRA-mediated neutrophil differentiation of NB4 control and Orlistat treated cells. H. Representative images of NBT assays in control and Orlistat treated NB4 cells upon ATRA-mediated differentiation. I. Quantification of the percentage of $NBT^+$ cells. J. Flow cytometry analysis of CD11b surface expression in NB4 control and Orlistat treated cells upon ATRA-mediated differentiation.

**Figure 5**: FASN expression is linked to increased mTOR activity. A-C. Autophagy induction in NB4 sh*FASN* cells treated with 1µM ATRA for 24h, in the presence or absence of BafA1 during the last 2h before harvesting. A-B. NB4 control (SHC002) and FASN knockdown (shFASN_1, _2) cells were subjected to LC3B immunofluorescence. A. Representative picture of LC3B punctae in NB4 control (SHC002) and FASN knockdown (shFASN_1, _2) cells. B. Quantification of autophagy flux. Three independent experiments were quantified as described in [85]. C. Total protein was extracted and submitted to immunoblotting using anti-LC3B and anti-p62 antibodies. Total protein is shown as loading control. Relative protein expressions were normalized to total protein and quantified using ImageJ software (NIH, Bethesda, MD, USA) D. NB4 control (SHC002) and FASN knockdown (shFASN_1, _2) cells were treated for 1 to 3 days with ATRA. Total protein was extracted and submitted to immunoblotting using anti-FASN, anti-pmTOR(Ser2448), anti- pULK1(Ser757), anti-ULK1, anti-pATG13(Ser318) and anti-ATG13 antibodies. E-F. Relative protein expressions of two independent experiments were normalized to total protein or the respective non-phosphorylated protein and quantified using ImageJ software (NIH, Bethesda, MD, USA). E. pmTOR(Ser2448) normalized to total protein. F. pULK1(Ser757) normalized to total ULK1. G. pATG13(Ser318) normalized to total ATG13.

**Figure 6**: FASN expression negatively associates with TFEB activity. A. Heatmaps of the correlation between FASN and TFEB target genes extracted from the TCGA-AML cohort analyzed by the UCSD xena platform and from the bloodspot data bank (Spearman, p values in Supplementary Table1 and 2). B. mRNA sequencing data of NB4 cells treated with ATRA. Relative expression of FASN, TFEB and TFEB transcriptional targets involved in lysosomal function and biogenesis are shown. C-H. NB4 control (SHC002) and FASN knockdown (shFASN_1, _2) cells were treated for 1

to 3 days with ATRA. (C) Immunofluorescence microscopy of endogenous TFEB (red) and α-tubulin (green). IgG staining was used as negative control. Nuclei were stained with DAPI (blue). (D) Immunofluorescence microscopy of endogenous LAMP1 (red). Nuclei were stained with DAPI (blue). (E) LAMP1 punctae quantification of cells shown in D. (F-H) Acridine Orange staining. (F) Histogram representation of the ratio between RED and GREEN of NB4 control (SHC002) cells treated as described in 6C. (G) Representative histogram of NB4 control (SHC002) and FASN knockdown (shFASN_1, _2) cells treated as in 6C. (H) Overton percentage positive quantification of the RED/GREEN ratio of NB4 control (SHC002) and FASN knockdown (shFASN_1, _2) cells treated with ATRA at indicated times.

**Figure 7**: EGCG treatment accelerates TFEB translocation to the nucleus and improves lysosome biogenesis. NB4 and HT93 APL cells were treated for 1 to 3 days with ATRA in combination with indicated concentrations of EGCG. Cells were then subjected to (A) Western blot analysis of FASN and pmTOR(Ser2448), (B) TFEB endogenous immunofluorescence, (C-D) LAMP1 endogenous immunofluorescence, and (E-G) Acridine Orange staining. B. Representative pictures of TFEB in NB4 cells treated with ATRA and different concentrations of EGCG. C. Representative pictures of LAMP1 in NB4 cells treated with ATRA and different concentrations of EGCG. D. LAMP1 punctae quantification in ATRA and EGCG treated cells at indicated time points. E. Histogram representation or the ratio between RED and GREEN of NB4 cells treated with EGCG at indicated time and concentration. F. Representative histogram of NB4 cells treated with EGCG and ATRA at indicated time points and concentrations. H. Overton percentage positive quantification of the RED/GREEN ratio of NB4 cells treated with DMSO (upper panel) or ATRA (lower panel) at indicated times and in combination with indicated EGCG concentrations.

**Figure 8**: Lowering FASN protein expression levels improves ATRA therapy in non-APL AML cells. A-H: MOLM-13 (A, C, D, G), and OCI-AML2 (B, E, F, H) cells were treated with ATRA and different concentrations of EGCG (5, 10, 15uM) for 3 days (n=3). (A-B) CD11b surface staining was analyzed by flow cytometry. Box blot represent the median fluorescence intensity (MFI) of CD11b positive cells. C-F. Acridine Orange staining. Analysis was performed as in Figure 7E-G. G-H. Total protein extracted from MOLM-13 and OCI-AML2 cells treated as in 8A/B were subjected to immunoblotting using anti-FASN, anti-pmTOR(Ser2448), anti-pULK1(Ser757), anti-ULK1, anti-pATG13(Ser318) and anti-ATG13 antibodies. I-R. MOLM-13 and OCI/AML2 were stably transduced with 2 independent shRNA targeting *FASN* (n=3) I-J.: FASN knockdown efficiency was validated in MOLM-13 (I) and OCI/AML2 (J) by western blotting. K-R. MOLM-13 and OCI/AML2 control and FASN knockdown cells was treated with ATRA for 3 days. (K-L) CD11b surface marker expression was analyzed as in A-B. (M-P) Acridine Orange staining analysis was performed as in 7E-G. (Q-R) Western blot analysis of Total protein was extracted and submitted to immunoblotting using anti-FASN, anti-pmTOR(Ser2448), anti-pULK1(Ser757), anti-ULK1, anti-pATG13(Ser318) anti-ATG13 and p4BPE1 antibodies.

Figure 1

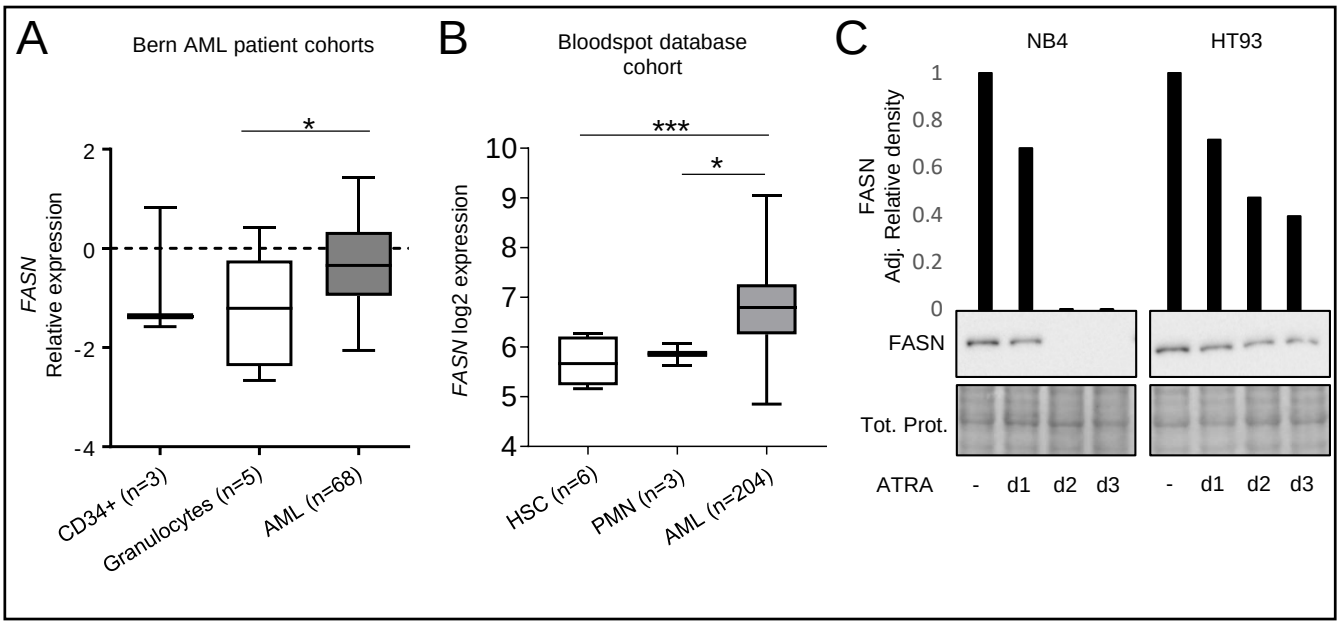
A
Bern AML patient cohorts
FASN Relative expression
2
0
-2
-4
*
CD34+ (n=3)
Granulocytes (n=5)
AML (n=68)
B
Bloodspot database cohort
FASN log2 expression
10
9
8
7
6
5
4
***
*
HSC (n=6)
PMN (n=3)
AML (n=204)
C
NB4
HT93
FASN Adj. Relative density
1
0.8
0.6
0.4
0.2
0
FASN
Tot. Prot.
ATRA - d1 d2 d3 - d1 d2 d3

Figure 2

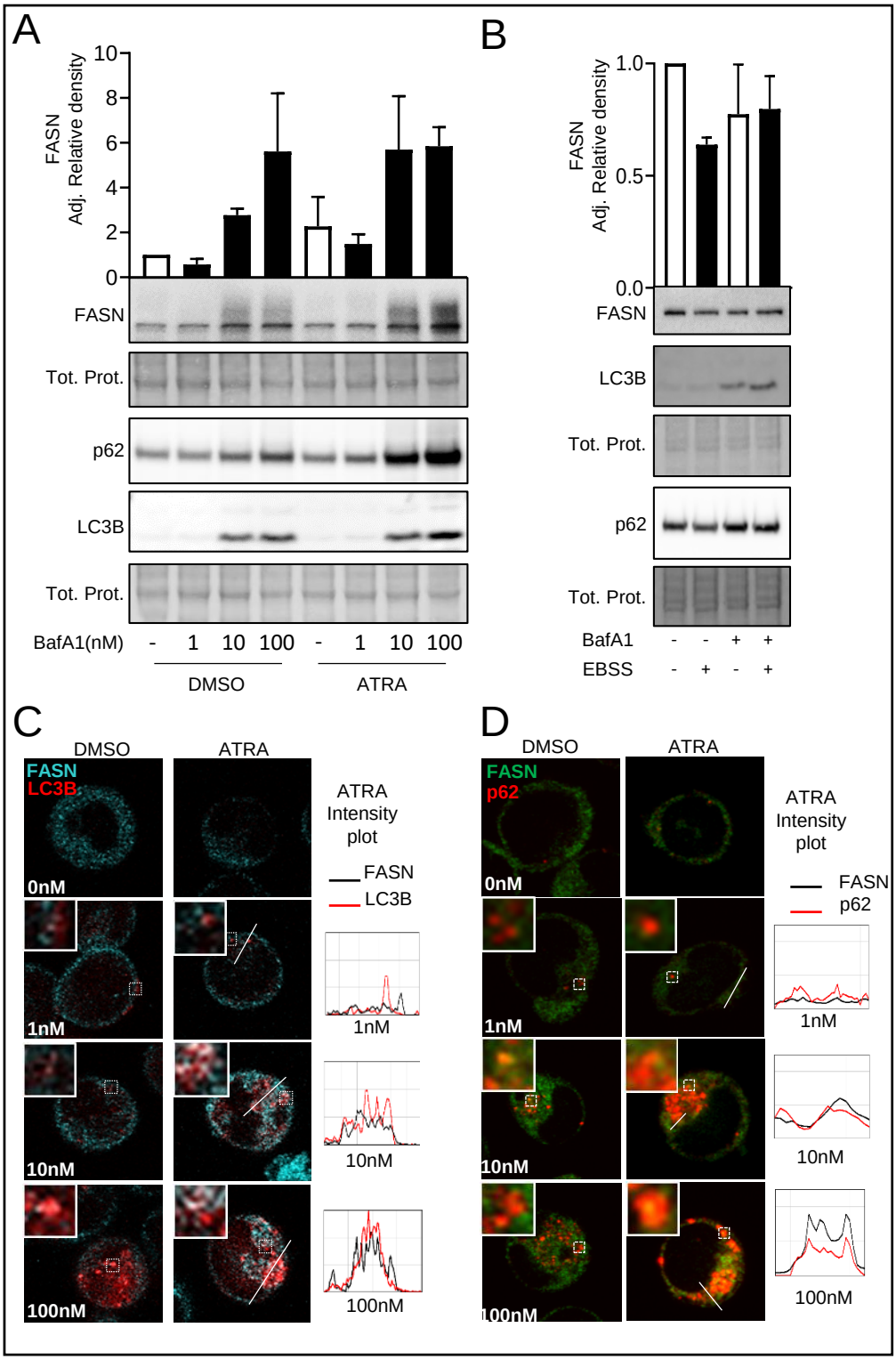
A
FASN
Adj. Relative density
10
8
6
4
2
0
FASN
Tot. Prot.
p62
LC3B
Tot. Prot.
BafA1(nM) - 1 10 100 - 1 10 100
DMSO
ATRA
B
FASN
Adj. Relative density
1.0
0.5
0.0
FASN
LC3B
Tot. Prot.
p62
Tot. Prot.
BafA1 - - + +
EBSS - + - +
C
DMSO
ATRA
FASN
LC3B
0nM
1nM
10nM
100nM
ATRA
Intensity
plot
FASN
LC3B
1nM
10nM
100nM
D
DMSO
ATRA
FASN
p62
0nM
1nM
10nM
100nM
ATRA
Intensity
plot
FASN
p62
1nM
10nM
100nM

Figure 3

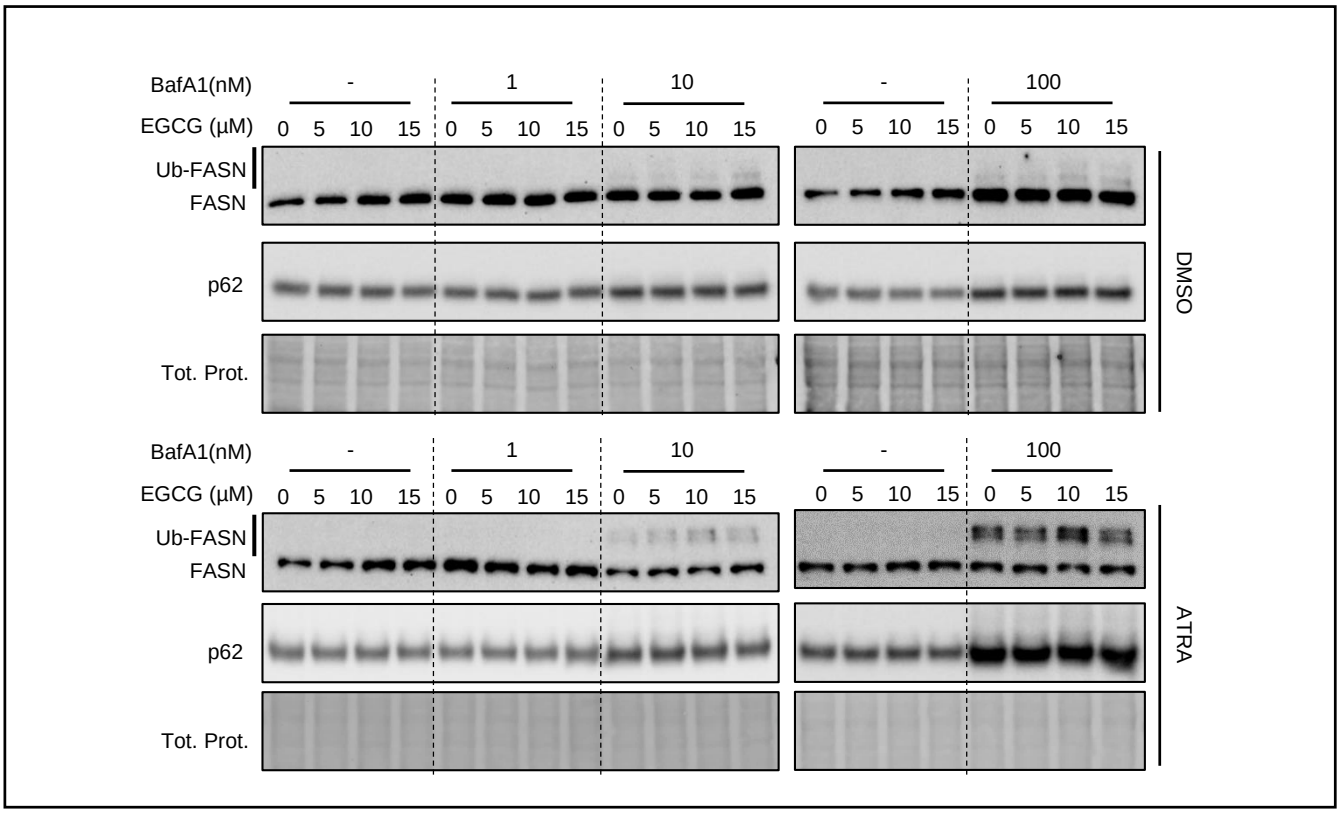
BafA1(nM)
-
1
10
-
100
EGCG (μM)
0 5 10 15 0 5 10 15 0 5 10 15 0 5 10 15 0 5 10 15
Ub-FASN
FASN
p62
Tot. Prot.
DMSO
BafA1(nM)
-
1
10
-
100
EGCG (μM)
0 5 10 15 0 5 10 15 0 5 10 15 0 5 10 15 0 5 10 15
Ub-FASN
FASN
p62
Tot. Prot.
ATRA

Figure 4

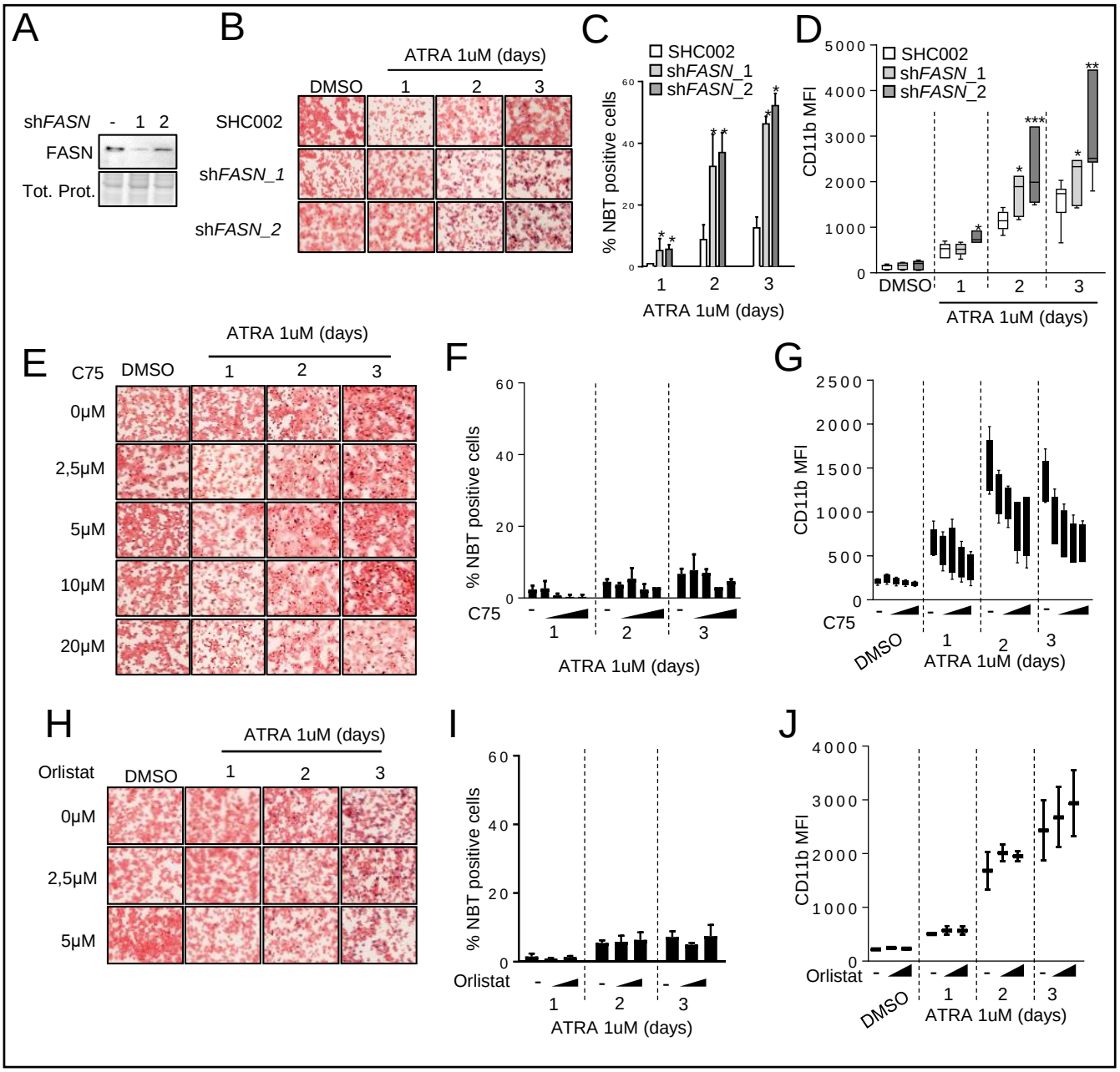
A
shFASN - 1 2
FASN
Tot. Prot.
B
ATRA 1uM (days)
DMSO 1 2 3
SHC002
shFASN_1
shFASN_2
C
SHC002
shFASN_1
shFASN_2
% NBT positive cells
ATRA 1uM (days)
D
SHC002
shFASN_1
shFASN_2
CD11b MFI
DMSO
ATRA 1uM (days)
E
ATRA 1uM (days)
C75 DMSO 1 2 3
0μM
2,5μM
5μM
10μM
20μM
F
% NBT positive cells
C75
ATRA 1uM (days)
G
CD11b MFI
C75
DMSO
ATRA 1uM (days)
H
ATRA 1uM (days)
Orlistat DMSO 1 2 3
0μM
2,5μM
5μM
I
% NBT positive cells
Orlistat
ATRA 1uM (days)
J
CD11b MFI
Orlistat
DMSO
ATRA 1uM (days)

Figure 5

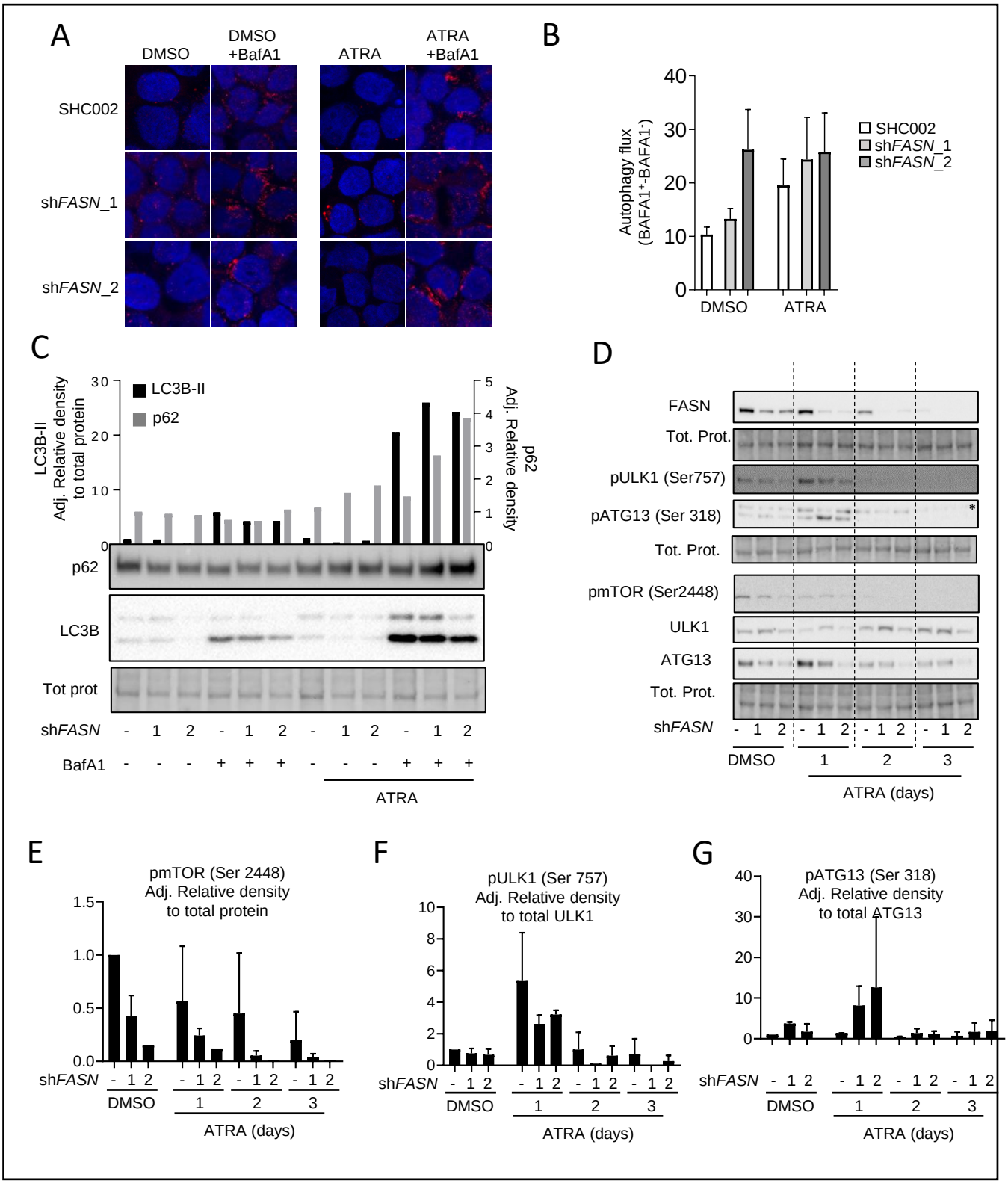
A
DMSO
DMSO +BafA1
ATRA
ATRA +BafA1
SHC002
shFASN_1
shFASN_2
B
Autophagy flux (BAFA1+-BAFA1-)
SHC002
shFASN_1
shFASN_2
DMSO
ATRA
C
LC3B-II Adj. Relative density to total protein
p62 Adj. Relative density
LC3B-II
p62
p62
LC3B
Tot prot
shFASN
BafA1
ATRA
D
FASN
Tot. Prot.
pULK1 (Ser757)
pATG13 (Ser 318)
Tot. Prot.
pmTOR (Ser2448)
ULK1
ATG13
Tot. Prot.
shFASN
DMSO
ATRA (days)
E
pmTOR (Ser 2448) Adj. Relative density to total protein
shFASN
DMSO
ATRA (days)
F
pULK1 (Ser 757) Adj. Relative density to total ULK1
shFASN
DMSO
ATRA (days)
G
pATG13 (Ser 318) Adj. Relative density to total ATG13
shFASN
DMSO
ATRA (days)

# Figure 6

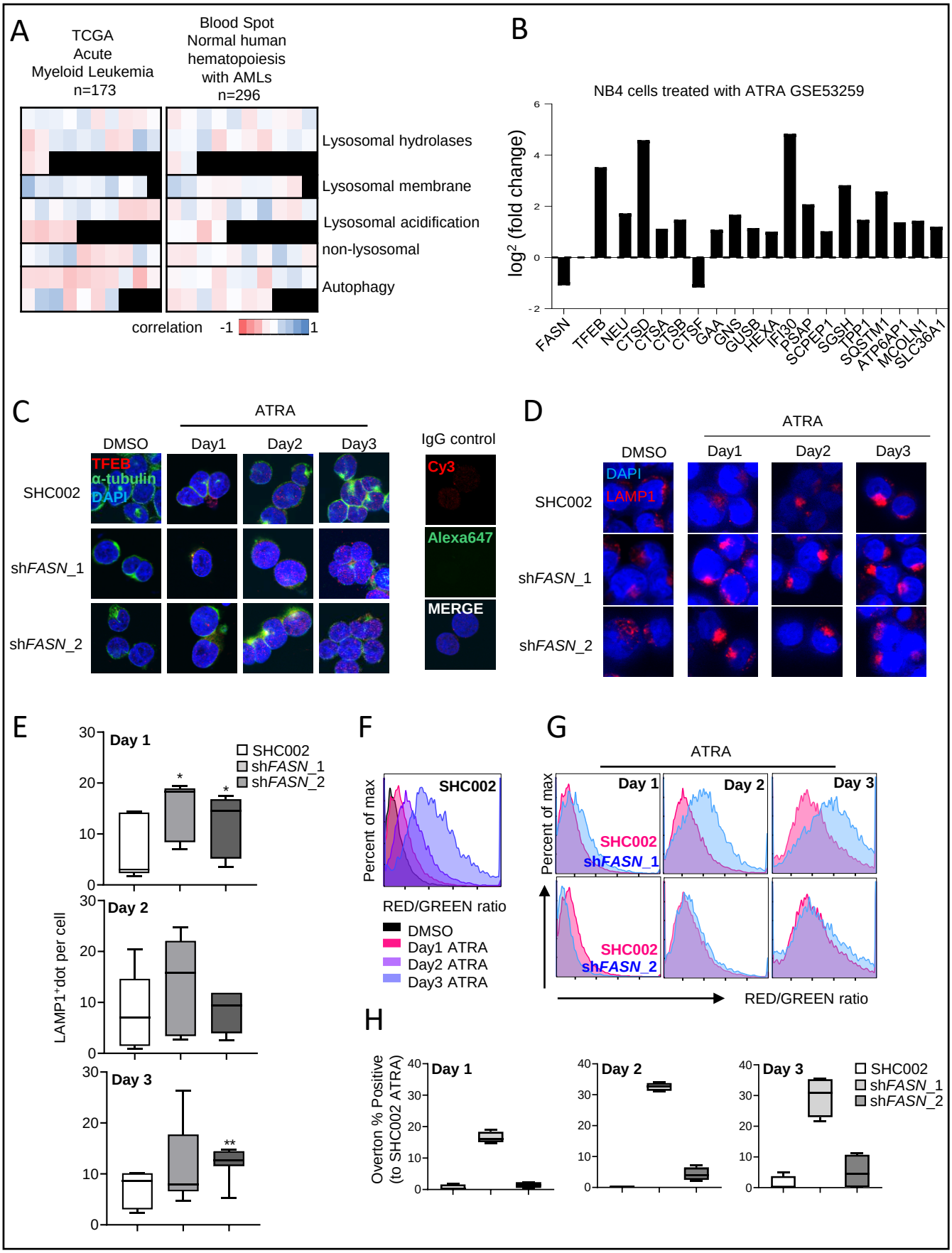
A
TCGA Acute Myeloid Leukemia n=173
Blood Spot Normal human hematopoiesis with AMLs n=296
Lysosomal hydrolases
Lysosomal membrane
Lysosomal acidification
non-lysosomal
Autophagy
correlation -1 1
B
NB4 cells treated with ATRA GSE53259
log2 (fold change)
FASN TFEB NEU CTSD CTSA CTSB CTSF GAA GNS GUSB HEXA IFI30 PSAP SCPEP1 SGSH TPP1 SQSTM1 ATP6AP1 MCOLN1 SLC36A1
C
ATRA
DMSO Day1 Day2 Day3
IgG control
SHC002
shFASN_1
shFASN_2
TFEB α-tubulin DAPI
Cy3
Alexa647
MERGE
D
ATRA
DMSO Day1 Day2 Day3
SHC002
shFASN_1
shFASN_2
DAPI LAMP1
E
Day 1
Day 2
Day 3
SHC002
shFASN_1
shFASN_2
LAMP1+dot per cell
F
SHC002
Percent of max
RED/GREEN ratio
DMSO
Day1 ATRA
Day2 ATRA
Day3 ATRA
G
ATRA
Day 1 Day 2 Day 3
Percent of max
SHC002
shFASN_1
SHC002
shFASN_2
RED/GREEN ratio
H
Overton % Positive (to SHC002 ATRA)
Day 1
Day 2
Day 3
SHC002
shFASN_1
shFASN_2

Figure 7

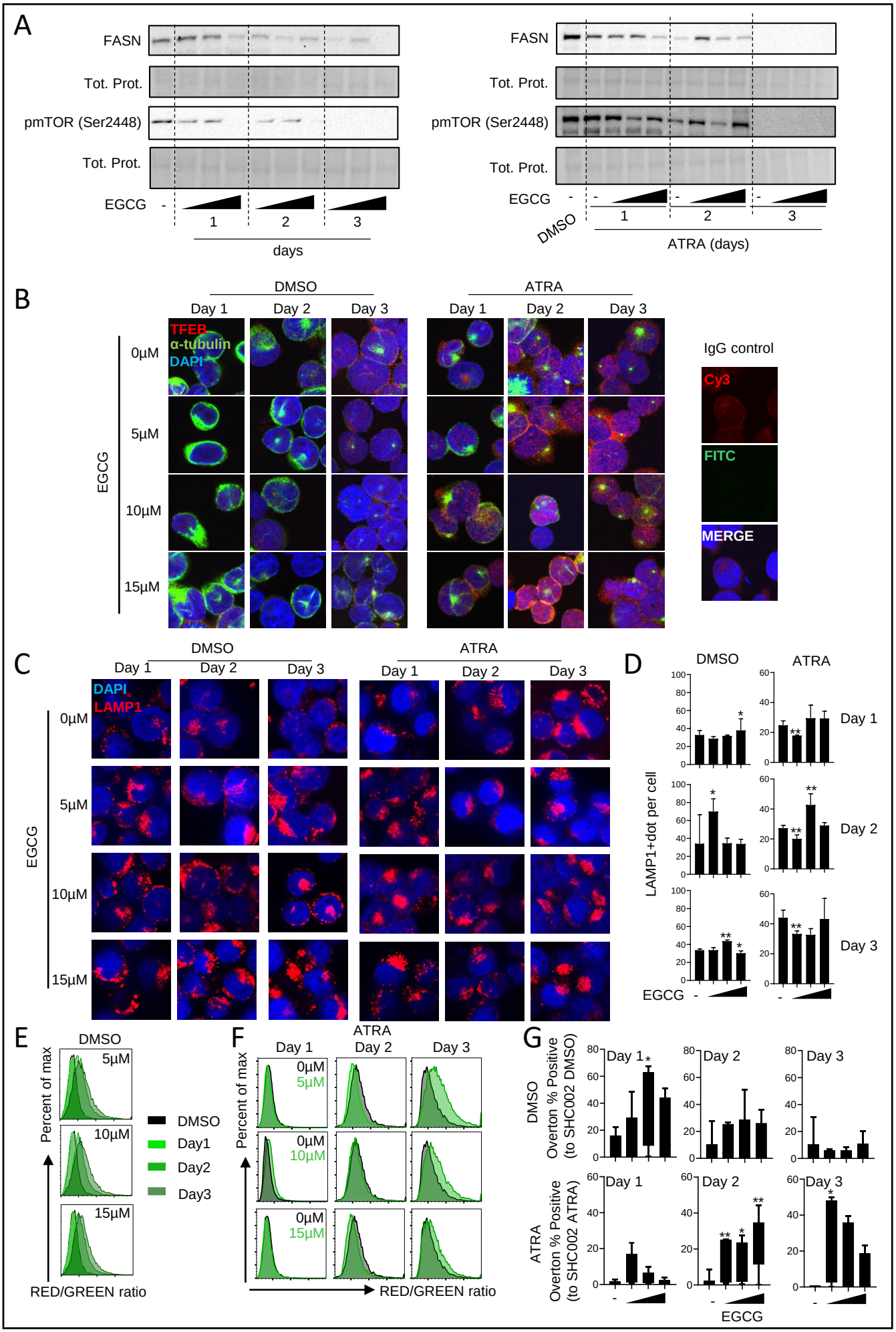
A
FASN
Tot. Prot.
pmTOR (Ser2448)
Tot. Prot.
EGCG
1
2
3
days
DMSO
ATRA (days)
B
DMSO
ATRA
Day 1
Day 2
Day 3
TFEB
α-tubulin
DAPI
0μM
5μM
10μM
15μM
EGCG
IgG control
Cy3
FITC
MERGE
C
DAPI
LAMP1
D
LAMP1+dot per cell
E
Percent of max
RED/GREEN ratio
DMSO
Day1
Day2
Day3
F
G
Overton % Positive (to SHC002 DMSO)
Overton % Positive (to SHC002 ATRA)

Figure 8

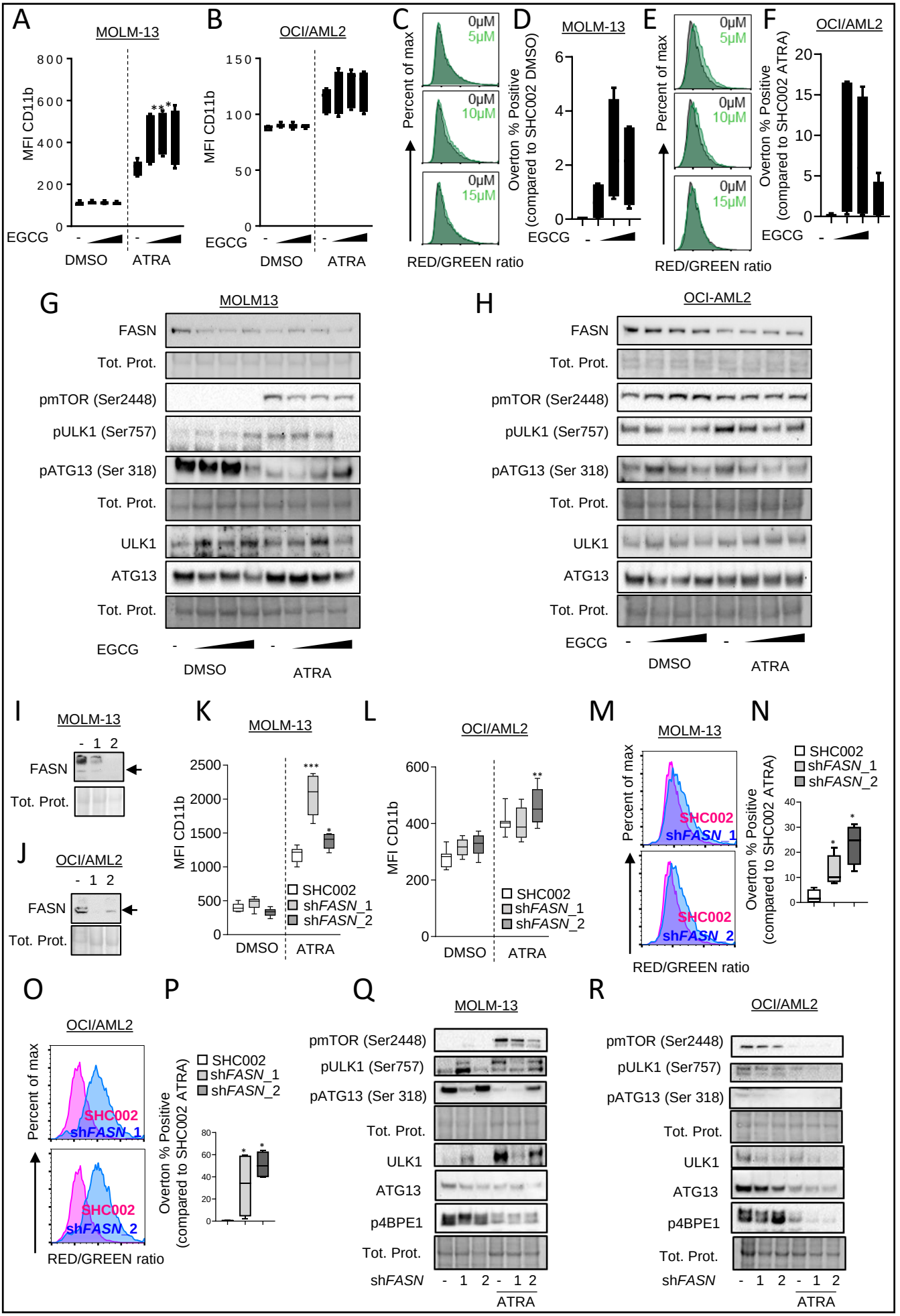
A
MOLM-13
MFI CD11b
800
600
400
200
0
EGCG
-
DMSO
ATRA
B
OCI/AML2
150
100
50
0
C
Percent of max
0μM 5μM
0μM 10μM
0μM 15μM
RED/GREEN ratio
D
MOLM-13
Overton % Positive (compared to SHC002 DMSO)
6
4
2
0
E
F
OCI/AML2
Overton % Positive (compared to SHC002 ATRA)
20
15
10
5
G
MOLM13
FASN
Tot. Prot.
pmTOR (Ser2448)
pULK1 (Ser757)
pATG13 (Ser 318)
ULK1
ATG13
H
OCI-AML2
I
MOLM-13
- 1 2
J
OCI/AML2
K
MOLM-13
2500
2000
1500
1000
500
0
SHC002
shFASN_1
shFASN_2
L
OCI/AML2
600
400
200
M
MOLM-13
SHC002
shFASN_1
shFASN_2
N
O
OCI/AML2
P
Q
MOLM-13
shFASN
ATRA
R
OCI/AML2